CHIN. PHYS. LETT. Vol. 28, No. 7 (2011) 074216

Photocurrent Effect in Reverse-Biased p-n Silicon Waveguides in Communication Bands *

ZHAO Yong(赵勇), XU Chao(徐超), WANG Wan-Jun(王皖君), ZHOU Qiang(周强), HAO Yin-Lei(郝寅雷), YANG Jian-Yi(杨建义), WANG Ming-Hua(王明华), JIANG Xiao-Qing(江晓清)**

Department of Information Science and Electronics Engineering, Zhejiang University, Hangzhou 310027

(Received 24 March 2011)

The photocurrent effect in reverse biased p-n silicon waveguides at wavelength 1550 nm is experimentally investigated. The photocurrent, which is mainly related to surface-state absorption, defect-state absorption and/or two-photon absorption, is more than 0.08 μA/mm under 8 V reverse biasing and 0.75 mW irradiation. The responsivity of a silicon waveguide with length of 4500 μm achieves 0.5 mA/W. Moreover, the enhancement of the photocurrent effect under the electric field is discussed.

PACS: 42.82.−m, 42.82.Et, 85.60.Gz DOI:10.1088/0256-307X/28/7/074216

Silicon photonics is a technology for implementing various optical functionalities in silicon, offering the potential for large-scale integration of multiple optical and electronic functions on a single silicon chip. Among optical functional devices, the photodetector is one of the key components. Silicon photodiodes are excellent detectors at visible wavelengths, but the development of high-performance silicon photodetectors at communication wavelengths has remained an imperative but unaccomplished task so far.[1] Thus it is an important issue to research and develop silicon photodetectors in communication bands.

Furthermore, it is known that silicon can generate photocarriers by utilizing surface-state absorption (SSA),[2,3] defect-state absorption (DSA)[4−6] and/or two-photon absorption (TPA)[7,8] in communication bands. Surface states naturally exist at silicon-air or silicon-silica interfaces. Yamashita *et al.*[9] measured the surface state density at silicon-silica interfaces, reporting that there are three density maxima at about 0.3, 0.5 and 0.7 eV above the valence-band maximum. Defects which always exist in semiconductors due to impurities or crystalline defects contribute energy states within the band gap.[10,11] For example, the divacancy has deep-level situated in the band gap 0.4 eV below the conduction band and such a light beam at 1550 nm may cause charge excitation from the valence band or the deep-level to the conduction band.[12] Thus both surface states and defect states introduce intermediate energy states in the band gap and make optical absorption extend to energies lower than the band gap energy ($E_g = 1.12$ eV). Different from SSA and DSA, TPA is a nonlinear absorption process. In a TPA process, two photons are absorbed simultaneously and an electron-hole pair is created. In this Letter, the photocurrent effect due to SSA, DSA and/or TPA in p-n silicon waveguides at a 1550 nm wavelength is presented. Photocurrents with different device lengths, reverse bias voltages and coupled optical powers are measured and discussed.

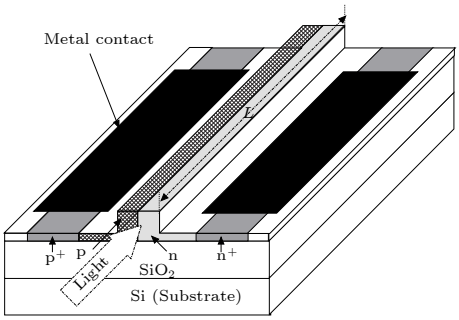

Fig. 1. Schematic digram of a silicon waveguide with a p-n diode.

The structure of a typical silicon waveguide with a p-n diode is shown in Fig. 1. This structure was fabricated on a silicon-on-insulator (SOI) wafer with a 340-nm-thick top silicon layer by a 0.18 μm CMOS process. The 400-nm-wide rib waveguide is implemented by etching 260 nm of the top silicon layer, with a 80-nm-thick silicon slab. The lightly doped regions (p and n, $2 \times 10^{17}/\text{cm}^3$) form a p-n junction in the waveguide core. The heavily doped regions (p^+ and n^+, $1 \times 10^{19}/\text{cm}^3$) both are 0.5 μm away from the edge of the waveguide. Metal is deposited on the heavily doped regions and etched to obtain electrodes. As shown in Fig. 1, L is the length of the p-n silicon waveguide.

The surface states and defect states are introduced naturally into the silicon waveguides, rather than intentionally by particular processes. Additionally, TPA can be potentially observed in silicon waveguides at wavelength 1550 nm because of the high optical power

*Supported by the Natural Basic Research Program of China under Grant No 2007CB613405, and the National Natural Science Foundation of China under Grant Nos 60977043 and 60808035.

**Correspondence author. Email: iseejxq@zju.edu.cn

© 2011 Chinese Physical Society and IOP Publishing Ltd

density and long interaction in silicon waveguides.[13] The photocarriers generated from SSA, DSA and/or TPA can be swept out of the depletion layer by an electric field and then forms the photocurrent.

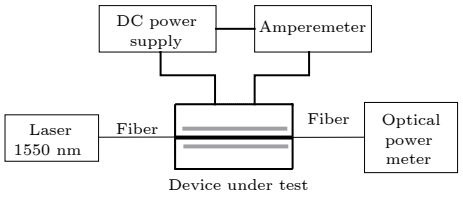

Fig. 2. Schematic diagram of the measurement setup.

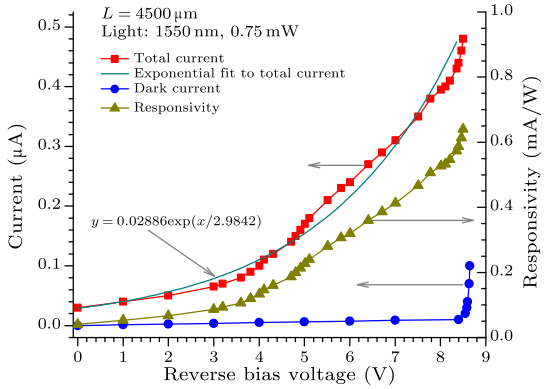

Fig. 3. I–V characteristic and responsivity of the device with $L = 4500\,\mu$m. The incident light is about 0.75 mW, at wavelength 1550 nm.

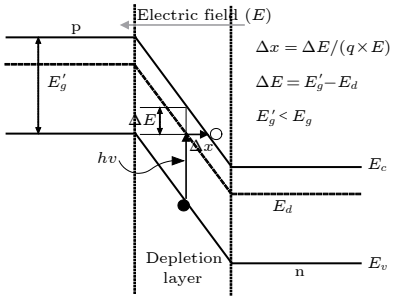

Fig. 4. Energy band diagram of the silicon p-n junction with an electric field.

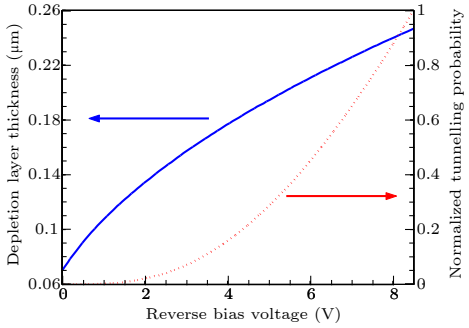

Fig. 5. Depletion layer thickness and normalized tunneling probability vs reverse bias voltage.

In our experiments, the 1550 nm light beam from a laser source (OPEAK, ASE Light Source) was coupled into the device under test by a grating coupler;[14] an amperemeter (Victor, VC9801A+) was in series with a dc power supply (Jiangbo, JBP-150) and the device. An optical power meter (ANDO, AQ8203) was used to monitor the optical at the output port for purpose of accurate coupling at the input port. Figure 2 schematically shows the measurement setup. When the reverse bias voltage or the coupled optical power is changed, different photocurrents can be obtained from the amperemeter.

The I–V characteristic and the responsivity of the device with L=4500 μm are shown in Fig. 3. The photocurrent and the responsivity increase with the reverse bias voltage. The reverse breakdown voltage is measured to be about 8.3 V, which is determined by the doping concentrations of $2 \times 10^{17}/\text{cm}^3$ in the p and n regions. The dark current, which is less than 0.02 μA under a reverse bias voltage lower than 8.3 V, is far below the total current. Thus it seems that most of the current is the photocurrent. Moreover, the photocurrent increases gently when the reverse bias voltage increases from 0 V to 3.5 V, but increases more significantly in the region from 3.5 V to 8.3 V. The increase of the photocurrent may be mainly due to two reasons. (1) The depletion layer thickness in the p-n junction increases with the reverse bias voltage.[15] The increase of the depletion layer thickness will introduce a larger overlap between the optical field and the depletion layer, and generate more photocarriers due to SSA, DSA and/or TPA. (2) Photon-assisted transition occurs more easily under higher electric field due to the tunnelling effect, as indicated in Fig. 4. The calculated electric fields in the depletion layer reach as high as 2.1×10^5 V/cm and 3.5×10^5 V/cm at 3.5 V and 8.3 V, respectively. When a strong electric field is applied to the silicon material, valence-band electrons can occupy states in the ordinarily forbidden region.[16] The introduction of the tunnelling states makes the band gap energy reduce from E_g to E_g'. Thus the electron will jump more easily to the intermediate state (E_d) by absorbing a photon $h\nu$. Furthermore, according to Fowler and Nordheim's theory,[17] electrons at E_d will tunnel through the barrier under electric field. The width of the barrier (Δx), as shown in Fig. 4, is inversely proportional to the magnitude of the electric field.[16] As shown in Fig. 5, the depletion layer thickness (the solid curve) has a square root relation with the reverse bias voltage.[15] The tunnelling probability (the dotted curve) follows an approximately exponential relation with the reverse bias voltage.[18] Additionally, it is known that the tunnelling current also presents an approximately exponential relation with the reverse bias voltage.[18] The measured photocurrent is coincident with the exponential fit curve from 3.5 V to 8.3 V, as illustrated in Fig. 3. Therefore, the increase of the photocurrent may be attributed mainly to the increase

of the depletion layer thickness from 0 V to 3.5 V and the electric-field-induced tunnelling effect from 3.5 V to 8.3 V.

It is obvious that a larger photocurrent can be obtained from a longer device because a longer waveguide can absorb more optical power and generate more photocarriers. We find that the experimental devices can present similar curves of photocurrent per mm length vs reverse bias voltage, as shown in Fig. 6. The value of photocurrent per mm length is greater than 0.08 μA/mm under 8 V reverse biasing and 0.75 mW irradiation.

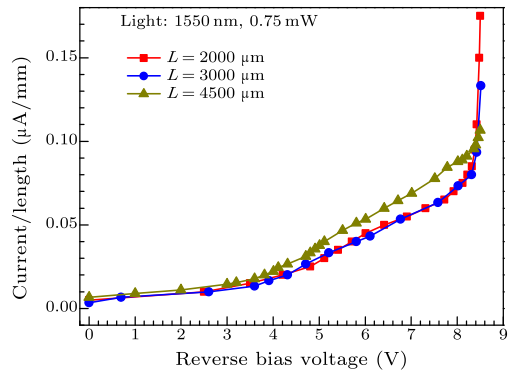

Fig. 6. Current per mm length vs reverse bias voltage. The incident light is about 0.75 mW, at the 1550 nm band.

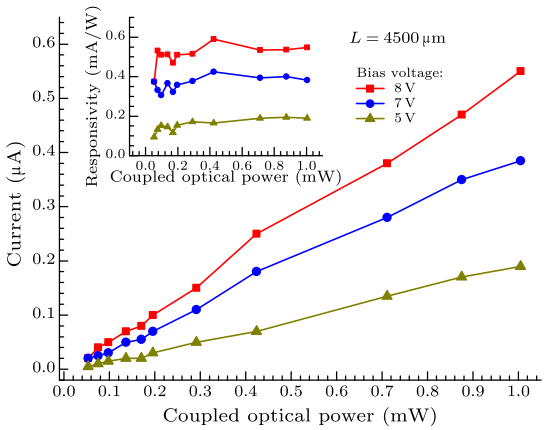

Fig. 7. Photocurrent vs coupled optical power at different reverse-bias voltages. Inset: responsivity vs coupled optical power at different reverse-bias voltages. The length of the device is 4500 μm.

Photocurrent and responsivity vs coupled optical power at different reverse-bias voltages are also considered. The photocurrent will show a quadratic dependence on the coupled optical power if TPA is dominant.[13] However, the photocurrents change linearly with the coupled optical power, while the responsivities are nearly constant, as illustrated in Fig. 7. Thus it seems that in our case, SSA and DSA contribute more to the photocurrents than TPA. The responsivity is about 0.5 mA/W under 8 V reverse biasing, which is about 3 times of that under 5 V reverse biasing.

In conclusion, we have investigated experimentally the photocurrent effect in reverse-biased p-n silicon waveguides to demonstrate the possibility of implementing silicon photodetectors at the 1550 nm communication band by employing SSA, DSA and/or TPA. The photocurrent achieves more than 0.08 μA/mm under 8 V reverse biasing and 0.75 mW irradiation. The responsivity of the p-n silicon waveguide with length of 4500 μm is about 0.5 mA/W under 8 V reverse biasing. Our experiments show that the photocurrent effect could be improved by increasing the length of the p-n silicon waveguide and the strength of the reverse-bias voltage. Furthermore, the photocurrent effect can also be enhanced by using resonant structures, such as microring resonators,[3,6] microdisk resonators[19] and photonic crystal cavities.[20]

References

[1] Casalino M, Coppola G, Iodice M, Rendina I and Sirleto L 2010 *Sensors* **10** 10571
[2] Baehr-Jones T, Hochberg M and Scherer A 2008 *Opt. Express* **16** 1659
[3] Chen H, Luo X and Poon A W 2009 *Appl. Phys. Lett.* **95** 171111
[4] Geis M W, Spector S J, Grein M E, Schulein R T, Yoon J U, Lennon D M, Deneault S, Gan F, Kaertner F X and Lyszczarz T M 2007 *IEEE Photon. Technol. Lett.* **19** 152
[5] Geis M W, Spector S J, Grein M E, Yoon J U, Lennon D M and Lyszczarz T M 2009 *Opt. Express* **17** 5193
[6] Preston K, Lee Y H D, Zhang M and Lipson M 2011 *Opt. Lett.* **36** 52
[7] Fathpour S, Tsia K K and Jalali B 2007 *IEEE J. Quantum Electron.* **43** 1211
[8] Bravo-Abad J, Ippen E P and Soljacic M 2009 *Appl. Phys. Lett.* **94** 241103
[9] Yamashita Y, Namba K, Nakato Y, Nishioka Y and Kobayashi H 1996 *J. Appl. Phys.* **79** 7051
[10] Fan H Y and Ramdas A K 1959 *J. Appl. Phys.* **30** 1127
[11] Cheng L J, Corelli J C, Corbett J W and Watkins G D 1966 *Phys. Rev.* **152** 761
[12] Logan D F, Jessop P E, Knights A P, Wojcik G and Goebel A 2009 *Opt. Express* **17** 18571
[13] Liang T K, Tsang H K, Day I E, Drake J, Knights A P and Asghari M 2002 *Appl. Phys. Lett.* **81** 1323
[14] Xiao X, Zhu Y, Xu H, Zhou L, Hu Y, Li Z, Li Y, Yu Y and Yu J 2010 *Chin. Phys. Lett.* **27** 094207
[15] Chuang S L1995 *Physics of Optoelectronics Devices* (New York: John Wiley)
[16] Wendland P H and Chester M 1965 *Phys. Rev.* **140** A1384
[17] Fowler R H and Nordheim L 1928 *Proc. R. Soc. London* A **119** 173
[18] Sze S M and Ng K K 2008 *Physics of Semiconductor Devices* (Xi'an: Xi'an Jiaotong University Press) (in Chinese)
[19] Chen H and Poon A W 2010 *Appl. Phys. Lett.* **96** 191106
[20] Bravo-Abad J, Ippen E P and Soljacic M 2009 *Appl. Phys. Lett.* **94** 241103